View metadata, citation and similar papers at core.ac.uk

brought to you by CORE

provided by Elsevier - Publisher Connector

Available online at www.sciencedirect.com

ScienceDirect

Energy Procedia 44 (2014) 234 – 243

Energy Procedia

E-MRS Spring Meeting 2013 Symposium D - Advanced Inorganic Materials and Structures for Photovoltaics, 27-31 May 2013, Strasbourg, France

Optimization of laser processes for local rear contacting of passivated silicon solar cells

M. Colina[a,]*, I. Martín[a], C. Voz[a], A. Morales-Vilches[a], P. Ortega[a], G. López[a], A. Orpella[a], M. García-Molina[a], D. Muñoz-Martín[b], M. I. Sánchez-Aniorte[b], C. Molpeceres[b] and R. Alcubilla[a]

[a]*Departament d'EnginyeriaElectrònica, Universitat Politècnica de Catalunya. C/ Jordi Girona 1-3, Mòdul C4, 08034 Barcelona, Spain*

**Use this author for all correspondence: Phone.: +34 93 401 74 88, Fax: +34 93 401 67 56, e-mail: monica.colina@upc.edu*

[b]*Centro Láser UPM, Universidad Politécnica de Madrid, Ctra de Valencia Km 7.3, 28031, Madrid, Spain*

Abstract

Laser Firing Contact (LFC) and Laser Doping (LD) have become potential alternatives to the Al BSF thermal processing conventionally used in p-type c-Si solar cell rear contacts. Optimized LFC and LD processes allow, not only the generation of efficient micro-contacts, but also the diffusion of p-type doping impurities reducing the surface recombination velocity due to the formation of a local back surface field (BSF). In this work, three different laser strategies to create ohmic micro-contacts are studied: *1)* evaporated Aluminum LFC, *2)* Aluminum foil LFC and *3)* Aluminum oxide (Al_2O_3) LD. The laser source used was a pulsed Nd-YAG 1064 nm laser working in the nanosecond regime. Laser parameters were explored to optimize the electrical behavior of the contacts and their carrier recombination rate. Optimized laser parameters lead to specific contact resistance in the 1.0 - 1.3 $m\Omega \cdot cm^2$ range for all three strategies. From the point of view of carrier recombination, better results were obtained for Al_2O_3 LD, probably related to the lower energy pulse needed to create the contact. Next, the three proposed laser approaches were applied to the back surface of heterojunction silicon solar cells. Contact quality was not limiting any cell performance indicating that the contact quality is good enough to be applied in high-efficiency c-Si cell concepts. On the other hand, surface recombination velocity at the rear surface on the final devices also points out to Al_2O_3 LD as the best alternative.

© 2013 The Authors. Published by Elsevier Ltd. Open access under CC BY-NC-ND license.

Selection and peer-review under responsibility of The European Materials Research Society (E-MRS)

Keywords: Laser Doping; Laser firing contact; crystalline silicon solar cells

1876-6102 © 2013 The Authors. Published by Elsevier Ltd. Open access under CC BY-NC-ND license.

Selection and peer-review under responsibility of The European Materials Research Society (E-MRS)

doi:10.1016/j.egypro.2013.12.033

1. Introduction

The use of the Laser-Fired Contact (LFC) technique to locally create Al-Si alloys in p type Passivated Emitter and Rear Cells (PERC) has been extensively studied for the creation of back contacts [1,2,3]. Different LFC approaches using Al sources as different as evaporated Al [1], screen printed Al [4] and Al foil [5] have been successfully tested, resulting in efficiencies between 18 and 22% even in industrially processed solar cells. In addition, different laser wavelengths and pulse durations have shown their potential to generate contacts with acceptable properties [6] making LFC a very flexible technology.

Recently, an alternative to LFC consisting in a laser-doping (LD) treatment has been proposed [7,8]. In this case, p-type atoms coming from an Aluminum oxide (Al_2O_3) rear passivation layer are diffused into the Si-base by the action of laser pulses while the dielectric film is simultaneously ablated. Hence, an optimized Al_2O_3 laser treatment leads to the formation of p-type doped regions which can be subsequently metalized for contact creation. A remarkable advantage of the LD technique is the lower energy required for the Al_2O_3 laser processing in comparison to the one required for the LFC processes [7,8], leading to a reduced damage on the Si-base.

In this work, three different laser contact strategies are compared: *1)* evaporated *Al LFC*, *2) Al foil LFC* and *3) Al_2O_3 LD*. For all the approaches, contact quality has been evaluated by means of specific contact resistance (ρ_{cef}) measurements. Additionally, the effective surface recombination velocity (S_{eff}) of surfaces treated by the three laser approaches has been estimated by means of minority carrier lifetime measurements and the application of the Fisher´s analytical model [9]. Finally, several p-type heterojunction solar cells have been prepared using the three laser contact strategies on their back surfaces. Internal Quantum Efficiency (IQE) measurements of the fabricated devices is used to calculate the effective diffusion length (L_{eff}) [10,11] and the back surface recombination velocity (S_{rear}). A comparison of the different S_{rear} values for every laser approach permits a reliable identification of the optimal laser treatment and its real impact on the performance in the final device.

Nomenclature

ρ_{cef}	specific contact resistance
S_{eff}	effective surface recombination velocity
L_{eff}	effective diffusion length
S_{front}	front surface recombination velocity
S_{rear}	back surface recombination velocity
S_c	effective contact recombination velocity
R_{LFC}	resistance between front and back surfaces
n	refraction index
f_c	laser treated area fraction
r	radius of the contact
R_s	spreading resistance
R_c	contact resistance
ρ_b	base resistivity
W	wafer thickness
τ_{eff}	effective lifetime
τ_b	volume lifetime
J	current density
V	voltage
V_{oc}	open-circuit voltage
Jsc	short-circuit current density
FF	solar cell fill factor
η	solar cell efficiency
α	absorption coefficient
D_b	bulk diffusivity

2. Experimental

2.1. Laser System and Samples

The laser system used for all the experiments was a Gaussian pulsed Nd-YAG lamp pumped laser (Starmark SMP100 II Rofin-Baasel) working at 1064 nm, with a pulse frequency of 4 kHz, a beam radius of 80 µm and two different pulse duration modes: 100 and 400 ns.

The substrates employed for sample preparation were Float Zone 2.5 Ω·cm p-type doped c Si wafers. Previous to the deposition of passivation layers, all the substrates were cleaned following a complete RCA sequence. Two types of passivation films were studied in this work: *1)* a 30 nm amorphous silicon carbide film with ×~0.2 (labeled as a-SiC_x:H PAS) deposited by PECVD at 300°C (direct plasma, 13.56 MHz ElectroRava S. p. A.), and *2)* a 50 nm Al_2O_3 film deposited by ALD at 200°C (Savannah S200, Cambridge Nanotech). In addition, an antireflective ($n = 2.0$) and dielectric amorphous silicon carbide with ×~1 (labeled as a-SiC_x:H ARC) film was deposited by means of PECVD at 300°C onto the passivating films, so as to complete a 100 nm stack. This thickness was determined to improve reflection at the back side of solar cells. Moreover, the addition of this antireflective layer results in a gentler laser-silicon interaction.

2.2. Effective contact resistance experiments

The three above-mentioned laser strategies were employed for the creation of micro contacts. Fig. 1 shows a scheme of the test samples to measure the quality of the contacts. In all cases, an evaporated Al layer was deposited onto the back surface creating an ohmic contact after an annealing in Forming Gas atmosphere at 375 ºC during 10 minutes. The resistance between the front and the back surface, R_{LFC}, was measured by means of the four wire sensing method after laser processing. An array of 3×3 micro contacts distributed in a 0.5 cm^2 area was prepared for each R_{LFC} measurement.

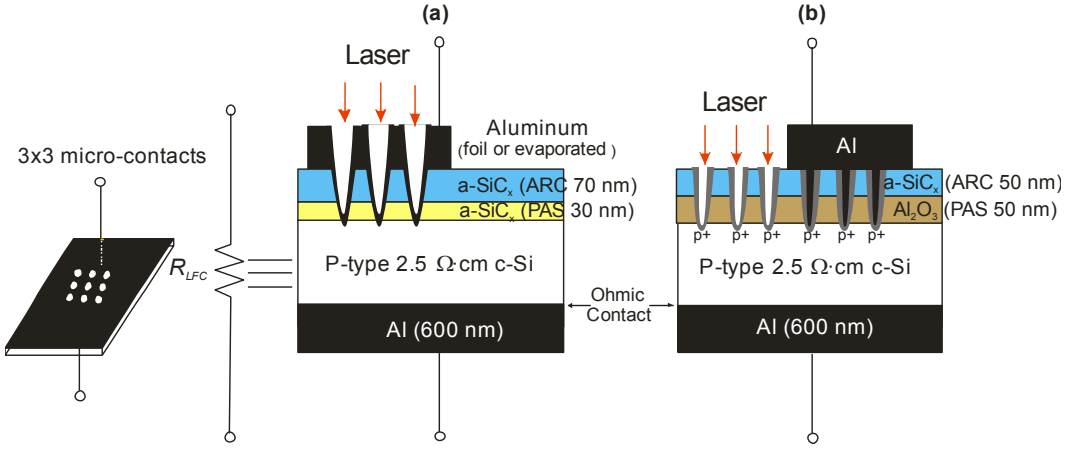

Fig. 1. Scheme of the samples used for the electrical characterization of the Laser micro-contacts (a) first and second laser contacting approaches; (b) third approach.

In the first laser strategy, micro-contacts are created by means of a burst of laser pulses impinging onto a thermally evaporated Al layer (Fig. 1a). This is the conventionally known as Laser Firing Contact (LFC) process, where laser pulses locally heat up the Al layer, the subsequent layers and the Si-base underneath, breaking the intermediate a-SiC_x:H(PAS)/a-SiC_x:H(ARC) stack and forming the micro-contact.

The second laser strategy replaces the evaporated Al layer by a 25 µm commercially available Al foil. In this case, previous to the LFC process, the foil must be arranged totally flat onto the c-Si avoiding air bubble

formation. This requirement is achieved by means of a flat chuck with a vacuum suction system which provides a uniform contact between the foil and the wafer. After laser processing, the Al foil remains attached to the sample since the micro-contacts formed act also as welding points.

The third strategy is based on the laser treatment of the Al_2O_3/a-SiC_x:H ARC stack (Fig. 1b). In this case, the laser treatment directly breaks the PAS/ARC stack and creates p-type doped regions in the c-Si. Thus, Al atoms coming from the Al_2O_3 layer dope the silicon underneath, which is then ready for the subsequent deposition of a metal for contact formation.

2.3. Surface recombination velocity experiments

A set of samples, whose structures are shown in Fig. 2, was prepared to determine the effective surface recombination velocity at the contacts, S_c, for every strategy. This magnitude can be deduced from minority carrier lifetime measurements which were done based on photoconductance technique (Sinton WCT-120). Samples corresponding to Fig. 2a were divided into two separated groups: *1)* evaporated *Al LFC* and *2) Al foil LFC*; while samples corresponding to Fig. 2b were directly treated by the third laser strategy: *Al_2O_3 LD*.

The experiment consisted in the creation of a 2×2 cm^2 array of micro-contacts that were obtained by the impinging of a burst of pulses onto the surface. The distance between contacts (or pitch) was varied in each sample leading to different laser treated area, f_c, defined as:

$$f_c = \pi\left(\frac{r}{pitch}\right)^2 \times 100\% \tag{1}$$

where r is the radius of the contact.

Four different f_c were tested for each laser approach. After the laser processing, metal was chemically removed for the evaporated *Al LFC* group and mechanically stripped for the *Al foil LFC* group. Finally, the dependence of the minority carrier lifetime on f_c was measured.

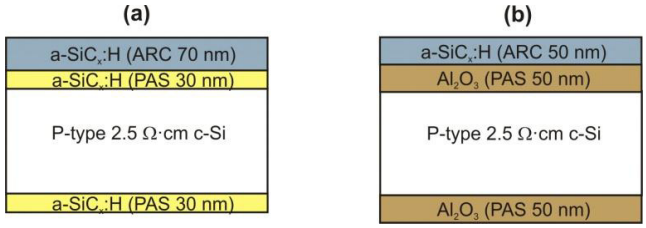

Fig 2. Structure of the test samples used for the determination of the contact surface recombination velocity for: (a) LFC strategies and (b) LD strategy.

2.4. Heterojunction solar cells

In order to compare the three laser approaches in a final solar cell device, heterojunction solar cells have been prepared on p-type 2.5 Ω·cm wafers according to the diagrams shown in Fig. 3. Dark and illumination (100 mW/cm^2, AM1.5g) J-V characteristics have been measured at 25 ºC for all the prepared devices. In addition, External Quantum Efficiency (EQE) and reflectance measurements were carried out by means of an EQE measurement system (QEX10 PV Measurements) and an UV-Vis-NIR spectrometer (Shimadzu 3600) respectively.

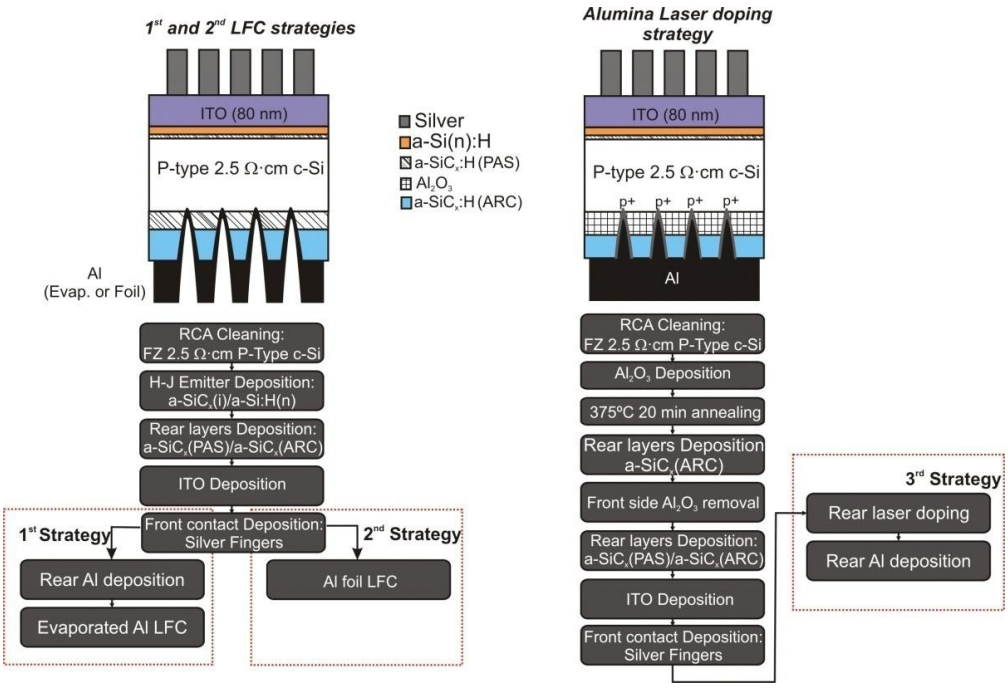

Fig 3. Diagram of the fabrication process of the heterojunction solar cells showing the three strategies proposed for the creation of the back contacts.

3. **Results and Discussion**

3.1. Laser Contact Characterization

The laser fired contact resistance, R_{LFC}, described in Fig. 1, was measured for samples treated according to the three above-mentioned laser strategies (evap. *Al LFC*, *Al foil LFC* and *Al_2O_3 LD*). Such resistance can be expressed as the sum of two terms, the spreading resistance, R_s, and the contact resistance, R_c. The spreading and the contact resistances can be calculated approximately as [3]:

$$R_s \cong (\rho_b / 2\pi r) tan^{-1}\left(2W/r\right) \tag{2}$$

$$R_c = \rho_{cef} / \pi r^2 \tag{3}$$

where ρ_b is the base resistivity, r is the contact radius, ρ_{cef} is the effective specific contact resistance and W is the c-Si wafer thickness.

The quality of the contacts is assessed by determining the ρ_{cef} value, i.e. the lower the ρ_{cef} value, the better the quality of the contact. Fig. 4 shows three optical images corresponding to typical laser contacts obtained using the three studied laser strategies. For the measurement of R_{LFC}, arrays of 3×3 laser micro-contacts were carried out onto each sample (see Fig. 1). Consequently, the resistance of a single contact was nine times the measured R_{LFC}. This approach reduces the impact of laser instabilities. In order to find the laser parameters leading to the lowest ρ_{cef} value, we experimentally determined that the most significant parameter on the electrical response is the laser

pulse power while the number of pulses and pulse duration play a minor role and were previously optimized. Fig. 5 shows the evolution of obtained ρ_{cef} values as a function of the pulse power for the three contacting strategies.

It can be observed that all the contacts exhibit low ρ_{cef} values between 1.0 and 10 mΩ·cm^2 with a clear minimum for every strategy. The best results were obtained for the evaporated *Al LFC* process with a ρ_{cef} value of about 1.0 mΩ·cm^2 while values of 1.1 and 1.2 mΩ·cm^2 were measured in the best cases for *Al foil LFC* and *Al_2O_3 LD* respectively. On the basis of these results, it can be stated that the three studied laser strategies allow the formation of good quality ohmic contacts without significant differences between them.

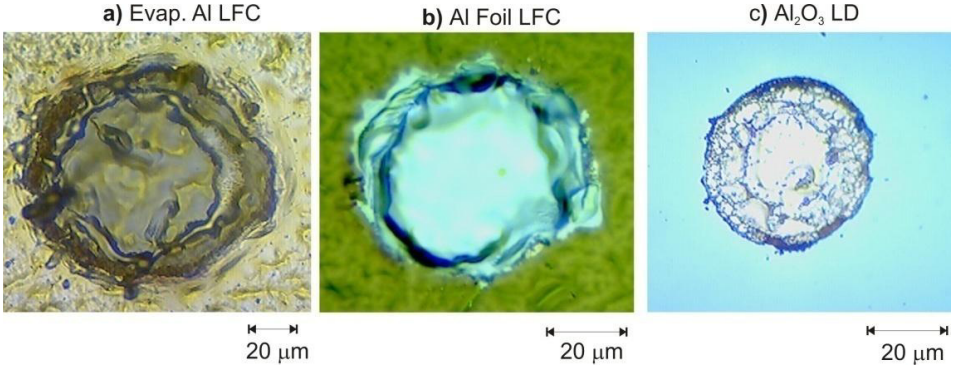

Fig 4. Optical image of a typical micro-contact created by: a) *Evap. Al LFC*, b) *Al foil LFC* and c) *Al_2O_3 LD*.

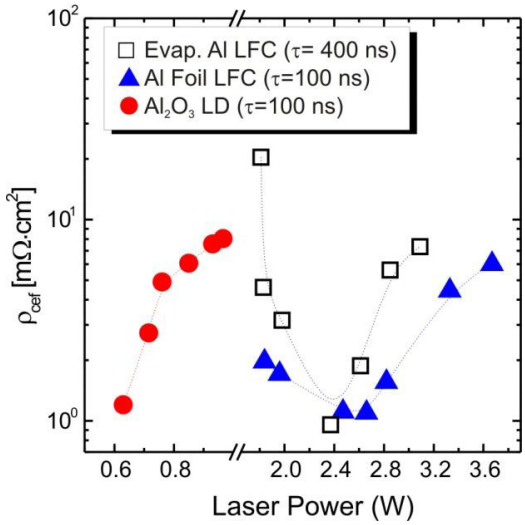

Fig 5. Results of the effective specific contact resistance ρ_{cef} as a function of the laser power for the three laser contacting strategies.

3.2. Effective surface recombination analysis

The loss of passivation in a surface treated by either LFC or LD can be estimated using effective lifetime, τ_{eff}, measurements. The effective surface recombination velocity, S_{eff}, of the laser treated surface is related to τ_{eff} according to the following expression:

$$\frac{1}{\tau_{eff}} = \frac{1}{\tau_b} + \frac{S_{front}}{W} + \frac{S_{rear}}{W} \quad (4)$$

where τ_b is the c-Si volume lifetime considering only intrinsic recombination processes modeled by ref.[12] and S_{front} and S_{rear} are the surface recombination velocities associated to the front and rear surfaces respectively. Laser treatment is performed on the front surface of each sample.

Before any laser treatment and assuming that the a-SiC_x:H ARC film does not impact on surface passivation, both surfaces have the same recombination velocity (S_{front} = S_{rear}) and can be calculated from lifetime measurements applying Eq. 4. Then, we laser processed the front surface of the samples according to procedure described in section 2.3 for four different laser-treated area fractions, f_c. The degradation of lifetime, i.e. the increase in S_{eff}, gives us information about the recombination at the laser-processed areas. Furthermore, Fischer's analytical model [9] allows us to calculate the effective recombination velocity at the contacts, S_c, created by the laser for every contact formation strategy.

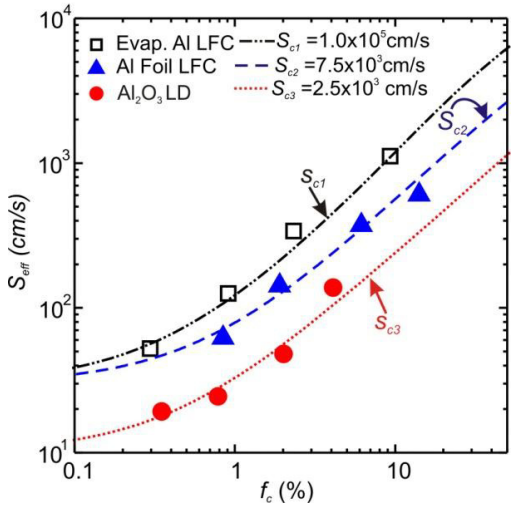

Fig 6. Effective surface recombination velocity as a function of the laser treated area fraction fc for the three laser contacting strategies.

Fig. 6 shows the experimental results and the analytical fittings. Table 1 shows a summary of the results obtained for the three laser strategies. The lowest S_c value is obtained for the *Al_2O_3 LD*, while evaporated *Al LFC* results in the worst contact passivation and *Al foil LFC* lies in-between. This could be related to the amount of laser power required to form the contacts, since it is about four times higher for both LFC techniques in comparison to Al_2O_3 doping (0.6 W for *Al_2O_3 LD* and 2.4-2.5 W for *LFC*). Thus, crystalline quality of the Si-base is more likely affected under LFC conditions than under *Al_2O_3 LD* conditions. The difference between both LFC techniques could be attributed to the thickness of Aluminum film (about 2 µm for *evap. Al LFC* and 25 µm for *Al foil LFC*) that attenuates the laser energy that reaches the c-Si bulk. Furthermore, an energy excess can presumably damage the passivation not only at the laser processed area, which is already expected, but also at its surroundings due to good lateral thermal conduction of c-Si.

Table 1. Summary of electrical characterization results of the optimal laser contacts.

Laser Contact Strategy	Laser Power (*W*)	ρ_{cef} ($m\Omega \cdot cm^2$)	Effective S_c (*cm/s*)
Evap. Al LFC	2.4	1.0	1×10^5
Al foil LFC	2.5	1.1	7.5×10^3
Al_2O_3 LD	0.6	1.2	2.5×10^3

3.3. Heterojunction solar cells analysis

Three series of heterojunction silicon solar cells were fabricated according to the structure shown in Fig. 3. The three described laser strategies were used to carry out the rear contact with a constant f_c of about 1% for all the

devices. Dark and light J-V curves under standard conditions were measured and a summary of the electrical results is shown in table 2.

Table 2. Summary of the electrical results of the heterojunction solar cells fabricated.

Laser contact strategy	# Cell	V_{oc} (*V*)	J_{sc} (mA/cm^2)	*FF* (%)	η (%)
Evap. Al LFC	1	0.626	29.0	73.68	13.27
	2	0.625	26.6	71.63	13.27
Al foil LFC	3	0.622	28.0	74.22	12.84
	4	0.629	30.0	71.12	13.22
Al_2O_3 LD	5	0.630	30.2	76.63	14.60
	6	0.625	31.5	75.35	14.82

The electrical results show similar open-circuit voltage (V_{oc}) and short-circuit current density (J_{sc}) values for all devices. However, fill factor (*FF*) and efficiency (η) values are remarkably better for the *Al_2O_3 LD* cells. The improved *FF* is linked to the shorter pitch used in the *Al_2O_3 LD* samples to maintain f_c at about 1%. In this case, the laser spot radius is only 25 µm leading to a pitch value of 450 µm, much shorter than the 1000 µm used for the LFC samples due to their bigger spot radii (~40 µm). In all cases, base resistivity is limiting the *FF* values in these cells and the contacts created by laser are of enough quality. This result agrees well with the high quality of the contacts determined in the previous section. Regarding J_{sc} and V_{oc} values, the similar values obtained suggest that recombination at the front amorphous/crystalline silicon interface is dominant. External Quantum Efficiency (EQE) measurements of the samples also point out to this conclusion. Then, in order to determine the rear surface recombination velocity, S_{rear}, in the final devices, we used the approach proposed by Basore [10,11] where the effective diffusion length of minority carrier along the c-Si bulk, L_{eff}, can be deduced from the IQE^{-1} vs. α^{-1} plot applying the following expression:

$$\frac{1}{IQE} = 1 + \alpha^{-1}\left(\frac{1}{L_{eff}}\right) \tag{5}$$

where α is the absorption coefficient. Then, S_{rear} can be calculated from the L_{eff} values using:

$$S_{rear} = \frac{D_b}{L_b} \times \frac{L_b - L_{eff} \cdot tanh\left(W/L_b\right)}{L_{eff} - L_b \cdot tanh\left(W/L_b\right)} \tag{6}$$

where L_b is the bulk diffusion length and D_b is the bulk diffusivity of minority carriers. Again, for the calculation of L_b we consider bulk lifetime values modeled by ref. [12].

Fig. 7 depicts the experimental data of IQE^{-1} vs. α^{-1} within the wavelength region $\lambda = 800\text{-}950$ nm for three different solar cells, each corresponding to one of the three laser contact strategies. The experimental data points were linearly fitted according to Eq. 5. The L_{eff} value for each device was obtained as the inverse of the slope for each linear fitting. Then, S_{rear} value for every solar cell was also calculated by applying Eq. 6.

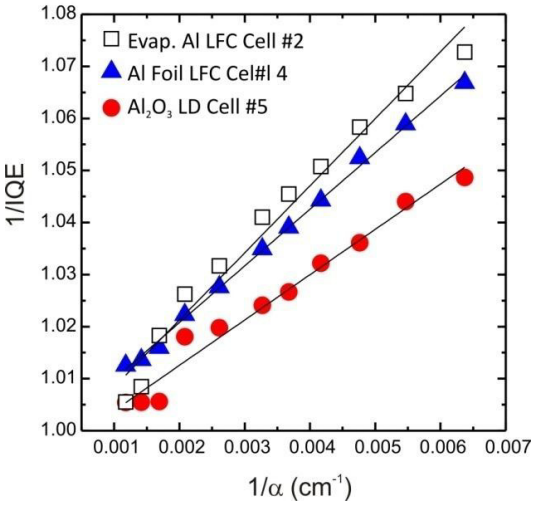

Fig 7. Inverse of the IQE vs. the inverse of the absorption coefficient α measured in heterojunction solar cells finished using the three proposed laser strategies for rear contacting.

Table 3 shows the calculated L_{eff} and S_{rear} results for the three laser strategies. From these results, it is confirmed that *Al_2O_3 LD* is the treatment that leads to the lowest recombination rate, while evaporated *Al LFC* results in the worst properties, giving evidence of significant damage. Although the results regarding the quality of the laser processes reproduce the ones deduced from the test samples, the S_{rear} values at the finished devices does not coincide with the S_{rear} values determined from the test samples, as it can be observed in table 3 where these last values are also included for direct comparison. This unexpected result can be attributed to different causes depending on the laser strategy used. For *Al_2O_3 LD*, a non-uniform doping distribution along the circular spot is expected with lower doping densities close to the spot edge. The subsequent back metallization of the doped micro-regions could lead to contact these low-doped regions shunting somehow the back surface field and resulting in higher surface recombination for the finished devices. Alternatively, for the LFC processes (both *Evap. Al LFC* and *Al foil LFC*) surface passivation is based on a SiC_x. It is well known that this type of layers have positive fixed charges that lead p-type c-Si surface to inversion conditions [13,14]. The presence of a metal film that contacts the base results in a short-circuit of this inversion layer increasing surface recombination. This effect has been reported for solar cells whose rear surface is passivated by silicon nitride films [14] where the positive fixed charge density is higher than SiC_x. All these effects that increase surface recombination in the finished devices could not be measured in the test samples since they have no metal and lifetime measurements are carried out under open-circuit conditions.

Table 3. Results of L_{eff} for the Heterojunction solar cells fabricated by the three different laser contacting strategies.

Laser Strategy	L_{eff} (*cm*)	S_{rear} (*cm/s*) in finished cells	S_{rear} (*cm/s*) in test samples
Evap. *Al LFC* : Cell #2	0.084	560	130
Al foil LFC : Cell #4	0.093	470	60
Al_2O_3 LD: Cell #5	0.131	300	25

4. Conclusions

Three different laser strategies were electrically compared and used to contact the back side of hetero-junction silicon solar cells: 1) *evap. Al LFC*, 2) *Al foil LFC* and 3) *Al_2O_3 LD*. Laser processed micro-contacts at optimum conditions exhibit specific contact resistance values around 1m$\Omega\cdot$cm^2, which is indicative of a high quality ohmic contact formation. Effective surface recombination velocity analysis on test samples led to the determination of the recombination velocity of the contacts created by the three laser strategies. Best results were obtained for *Al_2O_3 LD* with a S_c value of 2.5×10^3 cm/s. This is probably related to the much lower laser power needed to create the contacts. The electrical response of the hetero-junction silicon solar cells fabricated confirms that all three strategies are comparably efficient for the contact formation and that *Al_2O_3 LD* is the best technique from the point of view of surface recombination.

Acknowledgements

This work has been supported by the Spanish Ministry of Science and Innovation under projects ENE2010-21384-C04-04, TEC2011-26329, TEC2008-02520 and INNDISOL IPT-420000-2010-6 (FEDER funded "Una manera de hacer Europa").

References

[1] Schneiderlöchner E, Preu R, Lüdemann R, GlunzW. Laser-Fired Rear Contacts for Crystalline Silicon Solar Cells. Prog. In Photovol. 2002; 10: 29-34.
[2] Kray D, Glunz S. Investigation of laser-fired rear-side recombination properties using an analytical model. Prog. In Photovol. 2006; 14: 195-201.
[3] Ortega P, Orpella A, Martín I, Colina M, López G, Voz C, Sánchez MI, Molpeceres C, Alcubilla R. Laser-fired contact optimization in c-Si solar cells. Prog. In Photovol. 2011; 20: 173-180
[4] Nekarda J, Stumpp S, Gautero L, Hörteis M, Grohe A, Biro D, Preu R. LFC on screen printed aluminum rear side metallization. Proc. of 24th EPVSEC 2009; 1441-1445.
[5] Nekarda J, Grohe A, Schultz O, Preu R. Aluminum foil as back side metallization for LFC cells. Proc. of 22th EPVSEC 2007; 1499-1501.
[6] Molpeceres C, Sánchez-Aniorte MI, Morales M, Muñoz D, Martin I, Ortega P, Colina M, Voz C, Alcubilla R. Influence of wavelength on laser doping and laser-fired contact processes for c-Si solar cells. Proc. of SPIE 2012; 8473: 847308-1.
[7] Ortega P, Martín I, López G, Colina M, Orpella A, Voz C, Alcubilla R. P-type c-Si solar cells base don rearside laser procesing of Al_2O_3/SiC_xstacks. Sol. Energ. Mat. Sol. 2012; 106: 80-83.
[8] Martín I, Ortega P, Colina M, Orpella A, López G, Alcubilla R. Laser processing of Al_2O_3/a-SiC_x:H stacks: a feasible solution for rear surface of high-efficiency p-type c-Si solar cells. Prog.InPhotovol. 2012; DOI: 10.1002/pip.2207.
[9] Fischer B. Loss analysis of crystalline silicon solar cells using photoconductance and quantum efficiency measurements. Dissertation, Universität Konstanz; 2003.
[10] Basore PA. Extended spectral analysis of internal quantum efficiency.Proc. of the 23rd IEEE PhotovoltaicsSpc. Conf., New York, 1993; 147-153.
[11] Spiegel M, Fischer B, Keller S, Bucher E. Separation of bulk diffusion length and back surface recombination velocity by improved IQE-Analysis. Proc. of the 28rd IEEE Photovoltaics Spc. Conf., Anchorage, 2000; 311-314.
[12] Kerr MJ, Cuevas A, Campbell P. Limiting efficiency of crystalline silicon solar cells dueto Coulomb-enhanced Auger recombination. Progr. In Photovol.: Research and Applications 2003; 11: 97–104.
[13] Martín I, Vetter M, Orpella A, Puigdollers J, Cuevas A, Alcubilla R. Surface passivation of p-type crystalline Si by plasma enhanced chemical vapor deposited amorphous SiC_x:H films. Appl. Phys.Lett. 2001; 79:2199-201.
[14] Suwito D, Roth T, Pysch D, Korte L, Richter A, Janz S, Glunz SW. Detailed study on the passivation mechanism of a-Si_xC_{1-x} for the solar cell rear side, Proc. of 23th EPVSEC, 2008; 1023-1028.
[14] Dauwe S, Mittelstädt L, Metz A, Hezel R. Experimental evidence of parasitic shunting in silicon nitride rear surface passivated solar cells. Progr. in Photovol.: Research and Applications 2002; 10: 271-8.